The Astrophysical Journal, 858:101 (9pp), 2018 May 10 https://doi.org/10.3847/1538-4357/aabcb9

The Diffuse Radiation Field at High Galactic Latitudes

M. S. Akshaya[1], Jayant Murthy[2], S. Ravichandran[1], R. C. Henry[3], and James Overduin[4]
[1] Department of Physics, Christ (Deemed to be University), Bengaluru 560 029, India; akshaya.subbanna@gmail.com, ravichandran.s@christuniversity.in
[2] Indian Institute of Astrophysics, Bengaluru 560 034, India; jmurthy@yahoo.com
[3] Henry A. Rowland Department of Physics and Astronomy, The Johns Hopkins University, Baltimore, MD 21218, USA; henry@jhu.edu
[4] Department of Physics, Astronomy and Geosciences, Towson University, Towson, MD 21252, USA; joverduin@towson.edu
Received 2017 October 9; revised 2018 March 28; accepted 2018 April 6; published 2018 May 11

Abstract

We have used *GALEX* observations of the north and south Galactic poles to study the diffuse ultraviolet background at locations where the Galactic light is expected to be at a minimum. We find offsets of 230–290 photon units in the far-UV (1531 Å) and 480–580 photon units in the near-UV (2361 Å). Of this, approximately 120 photon units can be ascribed to dust-scattered light and another 110 photon units (190 in the near-UV) to extragalactic radiation. The remaining radiation is, as yet, unidentified and amounts to 120–180 photon units in the far-UV and 300–400 photon units in the near-UV. We find that molecular hydrogen fluorescence contributes to the far-UV when the 100 μm surface brightness is greater than 1.08 MJy sr^{-1}.

Key words: dust, extinction – local interstellar matter – surveys – ultraviolet: general – ultraviolet: ISM

1. Introduction

The diffuse radiation at high latitudes is, by definition, a combination of the diffuse Galactic light (DGL) and the extragalactic background light (EBL). The largest component of the DGL at low latitudes is the light from stars in the Galactic plane scattered by interstellar dust (Jura 1979), but this will be at a minimum at the poles, where there is little dust. Thus much of the diffuse light at the poles might be expected to be from the EBL (Bowyer 1991; Henry 1991). As a result, there have been many observations of the cosmic ultraviolet background at the pole and we have listed them in Table 1. The typical surface brightness was 200–300 photons cm^{-2} s^{-1} sr^{-1} Å^{-1} (hereafter photon units) in the far-ultraviolet (FUV: 1300–1800 Å) and 300–600 photon units in the near-ultraviolet (NUV: 1800–3200 Å).

The EBL is comprised of several parts with the most significant being the integrated light of galaxies, which Driver et al. (2016) found to be 60–81 photon units (FUV) and 121–181 photon units (NUV). These values are model-dependent but differ by no more than about 20 photon units (Gardner et al. 2000; Xu et al. 2005; Voyer et al. 2011). There may be smaller contributions from the integrated light of QSOs (16–30 photon units: Madau 1992) and the intergalactic medium (<20 photon units: Martin et al. 1991) for a total EBL of 96–131 photon units in the FUV and 157–231 photon units in the NUV. Phenomenological models of the cosmic spectral energy distribution are increasingly consistent with observational data and semi-analytic models, except in the ultraviolet, where they differ by as much as 100 photon units (see Figure 9 of Andrews et al. 2018). A good review of the current state of uncertainty in ultraviolet EBL intensity may be found in Figure 5 of Hill et al. (2018).

Henry et al. (2015) have argued strongly that there is an additional component to the DGL, unrelated to dust-scattered starlight. Much of the evidence for this component comes from *GALEX* observations of the Galactic poles in the FUV from Murthy et al. (2010). We have used an improved reduction of the diffuse background (Murthy 2014a) with a Monte Carlo model for the dust-scattered light (Murthy 2016) to further explore the background in the vicinity of both Galactic poles in the FUV (1531 Å) and the NUV (2361 Å).

2. Data

The *GALEX* mission (Martin et al. 2005; Morrissey et al. 2007) took observations covering most of the sky in the FUV and NUV bands. An observation consisted of one or more visits with exposure times of 100–1000 s each, which could be added together to reach total integration times of as long as 100,000 s. The original data from the mission were distributed as FITS (Flexible Image Transport System) files with a pixel size of 1.″5. Murthy (2014a) masked out the stars, rebinned to 2′ pixels and subtracted the foreground emission (Murthy 2014b) to produce a map of the diffuse background over the sky. We have used the visit-level data from Murthy (2014a), available from the High Level Science Products (HLSP) data repository[5] at the Space Telescope Science Institute, to study the diffuse emission at the Galactic poles.

We further rebinned the original 2′ bins of Murthy (2014a) by a factor of 3 (into 6′ bins) to improve the signal-to-noise ratio and the resultant maps are shown for the north Galactic pole (NGP) in Figure 1 and the south Galactic pole (SGP) in Figure 2 along with the 100 μm maps from Schlegel et al. (1998), also rebinned to 6′ pixels. Although one might expect a good correlation between the FUV and the NUV, and between both UV bands and the IR (Hamden et al. 2013; Murthy 2014a), there is much less structure in the NUV image than in the 100 μm images or, indeed, in the FUV.

Given that these are archival data, the number of visits and the exposure times per field fluctuate wildly but with most of the field observed in multiple visits. The deepest observation was the Subaru Deep Field (Kashikawa et al. 2004), which was targeted by *GALEX* (Ly et al. 2009) as part of the overall saturation coverage of that region by a number of different observatories. There were a total of 99 different visits in the FUV and 169 in the NUV with exposure times from 80–1700 s for each visit. The cumulative exposure times over the three years from 2004 April to 2007 May are 83,031 s in the FUV and 164,369 s in the NUV.

[5] https://archive.stsci.edu/prepds/uv-bkgd/

Table 1
Polar Observations

References	Wavelength (Å)	Offset (photon units)
Anderson et al. (1979)	1230–1680	285 ± 32
Paresce et al. (1979)	1350–1550	300 ± 60
Paresce et al. (1980)	1350–1550	<300
Joubert et al. (1983)	1690	300–690
	2200	160–360
Jakobsen et al. (1984)	1590	<550
	1710	<900
	2135	<1300
Tennyson et al. (1988)	1800–1900	300 ± 100
	1900–2800	400 ± 200
Onaka & Kodaira (1991)	1500	200–300
Feldman et al. (1981)	1200–1670	150 ± 50
Henry & Murthy (1993)	1500	300 ± 100
Murthy & Henry (1995)	1250–2000	100–400
Hamden et al. (2013)	1344–1786	300
Boissier et al. (2015)	1528	315
Murthy (2016)	1531	300
	2361	600

The primary source of uncertainty in the derived astrophysical background is the foreground emission (airglow in both bands and zodiacal light in the NUV), which is comparable to the astrophysical emission at high Galactic latitudes. We have tested the foreground subtraction by tracking the background surface brightness of a single 6′ bin over all the visits in the Subaru field (Figure 3). There are variations in both bands which, despite the missing FUV observations, are obviously correlated ($r = 0.9$). These are manifested as an increase in the overall background level of the image, which we believe is due to changes in the radiation environment around the spacecraft but we could not find any obvious trigger, either terrestrial or solar. The mean value of the background over all the visits in a 6′ pixel is 346 ± 41 photon units in the FUV and 563 ± 55 photon units in the NUV, and we have adopted these uncertainties in our analysis.

We took the individual visits and added them into polar grids (Figures 1 and 2), weighting each visit by its exposure time. Most of the field was covered by multiple visits, and we assumed that the diffuse surface brightness in a given field was comprised of a constant DGL + EBL with any difference between visits being due to the uncharacterized foreground discussed above. We subtracted this difference from each visit, effectively setting the median level of the diffuse surface brightness to the minimum over all visits.

There is a bright point in the top of the NUV image of the SGP (Figure 2) due to nebulosity around the fifth-magnitude star HD 224990 (B3V). We have not included those points in our analysis. Bright points in the FUV images are due to artifacts around hot stars and are not used in the analysis.

3. Results

3.1. UV–IR Correlations

Both the UV and the 100 μm surface brightness track the presence of dust and should be linearly correlated at high Galactic latitudes where the optical depth is low. We have

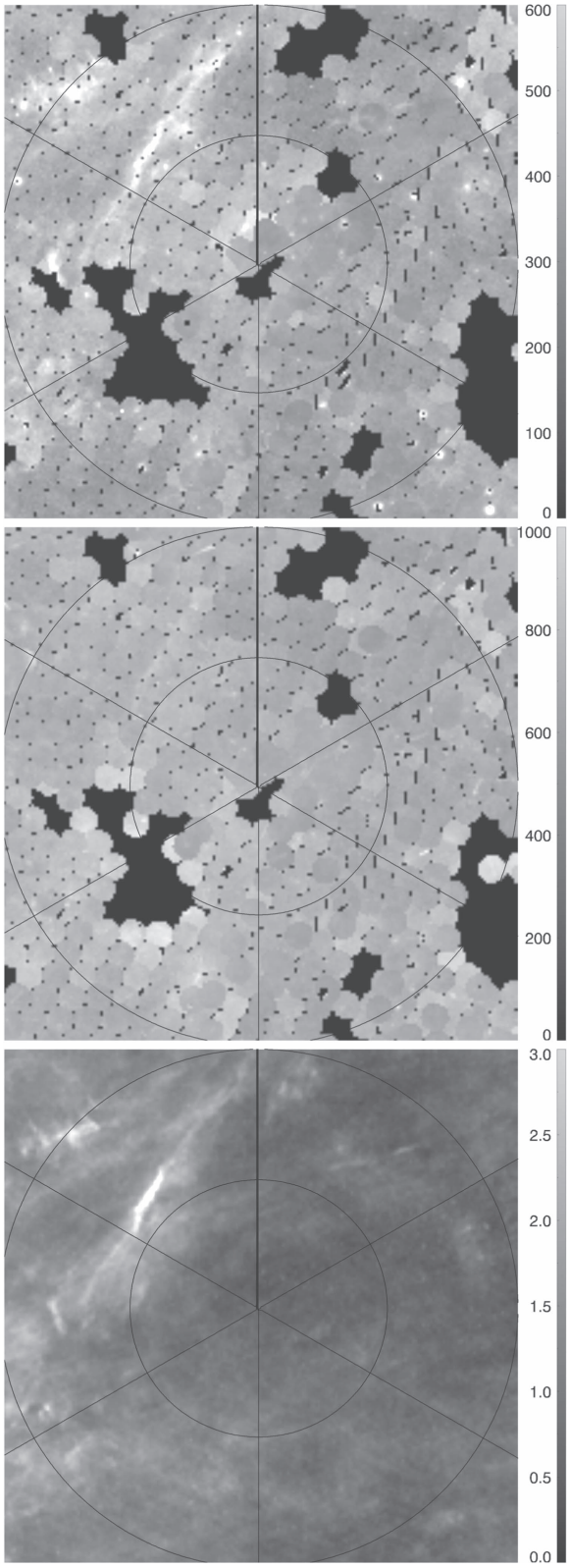

Figure 1. Observed surface brightness in the FUV (top) and NUV (middle) from *GALEX* and at 100 μm from Schlegel et al. (1998) (bottom). The FUV and NUV maps are in photon units and the 100 μm map is in MJy sr^{-1}. Black areas were not observed by *GALEX*. The NGP is at the center with lines of latitude at 80° and 85° and lines of longitude every 60° starting from 0° at the top increasing clockwise. Bright spots in the FUV image are due to artifacts around bright stars and were not included in the analysis.

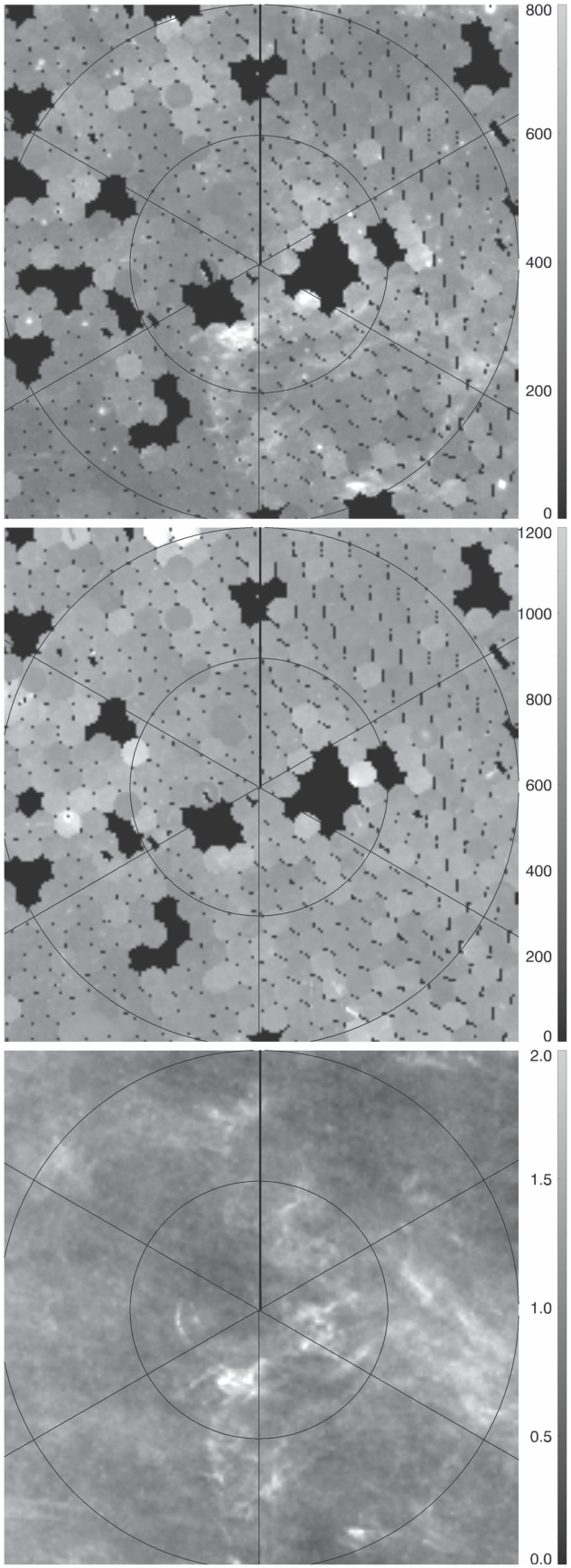

Figure 2. Same as in Figure 1 but for the SGP. The SGP is at the center with lines of latitude at −80° and −85° and lines of longitude every 60° starting from 0° at the top increasing anticlockwise.

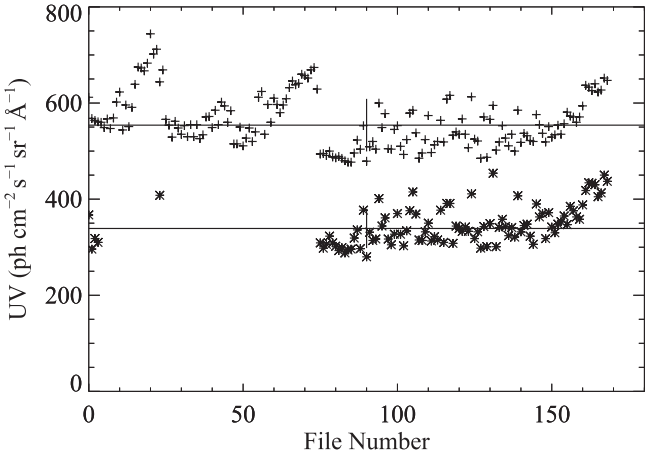

Figure 3. Median values for FUV (*) and NUV (+) in each visit. The horizontal lines show the medians in each band over all visits with the standard deviation plotted as vertical lines in the center of the plot. Many FUV values are missing because there were no observations on those dates.

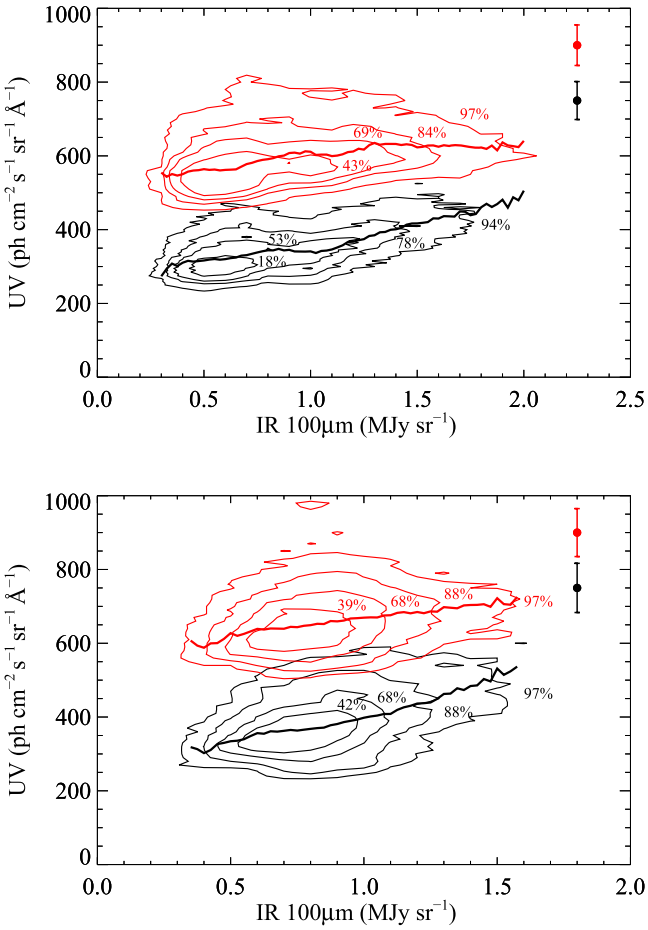

Figure 4. Contour plots of the FUV (black contours) and NUV (red contours) at the NGP (top) and SGP (bottom) where the IR bin size is 0.1 MJy sr^{-1} and the UV bin size is 5 photon units. We have shown the mean surface brightness in the UV averaged over bins of 0.025 MJy sr^{-1} in the IR. The error bars shown are representative of the standard deviation in the mean and are of the order of about 50 photon units for the NGP and 70 photon units for the SGP.

plotted the observed correlations in Figure 4 and tabulated them in Table 2. The UV does indeed correlate with the IR but not as well as one might expect, as is apparent from a visual comparison of the images in Figures 1 and 2. The bright IR

Table 2
Correlation Coefficients

Bands	p[a]	a[b]	b[c]	χ^2_ν
NGP				
FUV–IRAS	0.54	97.58	259.80	1.26
NUV–IRAS	0.42	68	530.89	1.18
FUV–$E(B-V)$	0.52	4245.40	250.11	1.24
NUV–$E(B-V)$	0.40	2655.67	531.06	1.21
SGP				
FUV–IRAS	0.42	164.17	240.99	2.29
NUV–IRAS	0.28	90.30	579.07	1.48
FUV–$E(B-V)$	0.45	7967.55	211.85	2.18
NUV–$E(B-V)$	0.29	4260.72	565.69	1.47
NGP (with inflection point)				
FUV–IRAS (<1.08 MJy sr^{-1})	0.27	57.43	288.27	1.15
FUV–IRAS (>1.08 MJy sr^{-1})	0.57	156.33	182.10	1.37

Notes.
[a] Spearman's correlation coefficient ($P \lll 0.05$ for all the cases).
[b] Scale factor.
[c] Offset (photon units).

features such as Markkanen's Cloud (Markkanen 1979) are readily seen in the FUV at both poles but are not prominent in the NUV.

We noted an inflection point in the FUV/IR ratio for the NGP at an IR surface brightness of 1.08 MJy sr^{-1} (Figure 5). We performed an *F*-test (Bevington & Robinson 2003) to investigate whether the additional term was justified and found an *F*-value of 1325, which is significant at a level greater than 99.9%. Matsuoka et al. (2011), perhaps coincidentally, found a similar inflection point at a 100 μm surface brightness of 0.8 MJy sr^{-1} in *Pioneer* optical data, which they identified with the cosmic infrared background (CIB: Lagache et al. 2000). In this scenario, both the CIB and the UV offset would represent the part of the background that is not correlated with interstellar dust. However, we would then expect a similar inflection point in the FUV data at the SGP or in the NUV at either pole, which is not seen.

Another possibility is that the change in slope is due to molecular hydrogen (H_2) fluorescence (Hurwitz 1998) in the Werner bands kicking in at a 100 μm surface brightness of 1.08 MJy sr^{-1} ($\log N_H = 20.2$, for N_H in units of cm^{-2}). Canonically, H_2 is only formed at column densities greater than $\log N_H = 20.5$–20.7 (Knapp 1974; Savage et al. 1977; Franco & Cox 1986; Reach et al. 1994), when self-absorption protects the molecules from dissociation by ultraviolet photons. Jo et al. (2017) have found that the fraction of the total diffuse radiation in the form of fluorescent Werner band emission from molecular hydrogen is 5%–10% of the total observed surface brightness at the poles, or about 30 photon units. These observations were averaged over 10°–15° at the poles, and we find that the putative Werner band emission in the *GALEX* data is about 60 photon units, not too far off from their observations. Gillmon et al. (2006) and Wakker (2006) have found significant molecular gas at high latitudes at column densities of $20.2 < \log N_H < 20.5$, which Gillmon et al. (2006) attributed to a clumpy medium with the molecular gas concentrated in high-density cirrus clouds. Unfortunately, we do not have the spectroscopic information needed to further investigate the emission and cannot further constrain the source of the rise in the FUV.

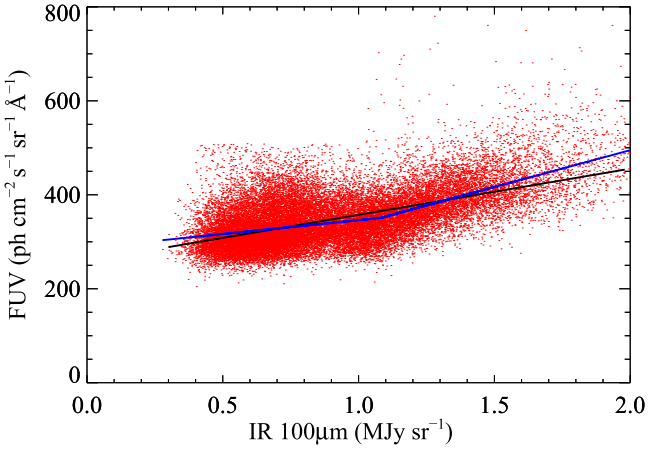

Figure 5. FUV surface brightness plotted against IR surface brightness for the NGP. The black line shows a linear fit over all the data points and the blue line shows the best fit with the inflection point at 1.08 MJy sr^{-1}.

3.2. Zero-points

The diffuse radiation at the poles is likely to be dominated by the EBL and the observed baseline will therefore place an upper limit on the EBL. The *y* intercepts for the FUV are 288 photon units for the NGP and 241 photon units for the SGP, with the corresponding values for the NUV being 531 and 579 photon units for the NGP and SGP, respectively. Taken at face value, these are upper limits for the EBL and match well with earlier determinations of the background at the poles (Table 1), including with *GALEX* results from Hamden et al. (2013), Boissier et al. (2015), and Murthy (2016). As an independent check, we have calculated the slopes and offsets using the $E(B-V)$ from Planck Collaboration et al. (2014), finding very similar offsets (Table 2). However, as discussed in the Introduction, the expected limits on the EBL are 96–131 photon units in the FUV and 157–231 photon units in the NUV, or about half the observed value in the FUV and about one third in the NUV. This offset has been noted before (Table 1) but with no definite identification (Henry et al. 2015).

3.3. Correlation with E(B – V)

Much of the *GALEX* Ultraviolet Virgo Cluster Survey (GUVICS: Boissier et al. 2015) falls within our area, and our extracted diffuse values are in excellent agreement in the areas of overlap, despite independent approaches to the extraction of the diffuse radiation from the *GALEX* observations. Boissier et al. (2015) subtracted what they termed "any emission not related to the cirrus" from the EBL and from unknown Galactic sources, possibly including "a very diffuse cirrus contribution," and then derived a linear relationship between the FUV (in photon units) and the reddening of $E(B-V) = 0.02378 + 8.77 \times 10^{-5} \times (\mathrm{FUV} - 315)$, where 315 photon units was their offset. They suggested that the diffuse UV background could be used to calculate the $E(B-V)$ at a higher spatial resolution and precision than either the *IRAS* data (Schlegel et al. 1998) or the *Planck* data (Planck Collaboration et al. 2014). This method does indeed show promise and we have attempted the same with our data over both poles (Figure 6) using *Planck* reddening. We found relations of

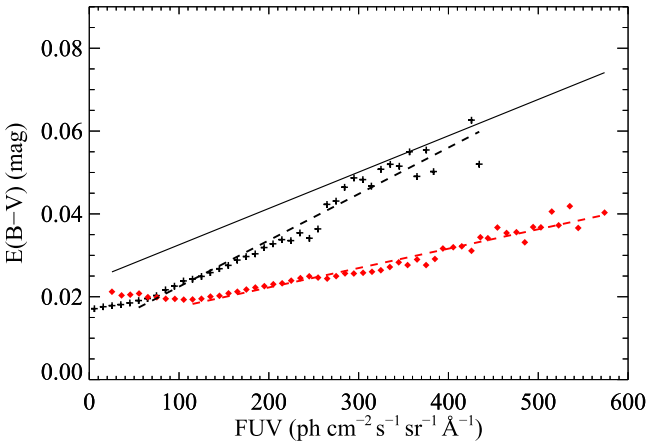

Figure 6. $E(B - V)$ from Planck Collaboration et al. (2014) plotted as a function of FUV for the NGP (plus signs) and the SGP (red diamonds), where the reddening has been averaged over the FUV bins. The straight line shows the relation derived by Boissier et al. (2015). The dashed lines show our best fit to the reddening for the NGP (black line) and the SGP (red line). Note that, in each case, an offset has been subtracted from the FUV to account for the non-cirrus emission.

$E(B - V) = 0.01124 + 1.119 \times 10^{-4} \times (\mathrm{FUV} - 250)$ over the much larger area we observe for the NGP and $E(B - V) = 0.01288 + 4.6841 \times 10^{-5} \times (\mathrm{FUV} - 212)$ for the SGP. As Boissier et al. (2015) point out, the FUV emission is dependent on the geometry of the stars and the dust, and care has to be taken when using the *GALEX* data to predict extinction over the sky.

4. Modeling Milky Way Radiation

Most of the DGL at low Galactic latitudes is unequivocally due to the scattering of the light of hot stars from interstellar dust, and we have applied the model developed by Murthy (2016) to predict the amount of Galactic dust-scattered radiation in the polar regions. This model uses a Monte Carlo process to track photons emitted from stars with location and spectral type from the *Hipparcos* catalog (Perryman et al. 1997) and stellar spectra from Castelli & Kurucz (2004). The dust was taken from the three-dimensional extinction map derived from PanSTARRS data by Green et al. (2015) with an angular resolution of about 14′ at the poles. The gaps in the map of Green et al. (2015) were filled using the reddening map given by Schlegel et al. (1998) with a scale height of 125 pc (Marshall et al. 2006). Our modeled dust distribution is shown in Figure 7 for the NGP and SGP and is similar to the IR maps shown in Figures 1 and 2, respectively. The distribution of the extinction with distance (along a specific line of sight) is shown in Figure 8 and is consistent with a scale height of 125 pc (Marshall et al. 2006) and a cavity of about 50 pc radius around the Sun (Welsh et al. 2010). We assumed the scattering function of Henyey & Greenstein (1941) with the albedo (a) and phase function asymmetry factor ($g = \langle \cos\theta \rangle$) as free parameters.

The dust at both poles has been extensively investigated through polarization measurements (Markkanen 1979; Berdyugin et al. 1995, 2000, 2001, 2004, 2011, 2014; Berdyugin & Teerikorpi 1997, 2002, 2016). The polarization at the NGP was divided into two regions: Area I and Area II (Markkanen 1979), approximately corresponding to the 100 μm surface brightness and the polarization being larger in Area II. The overall

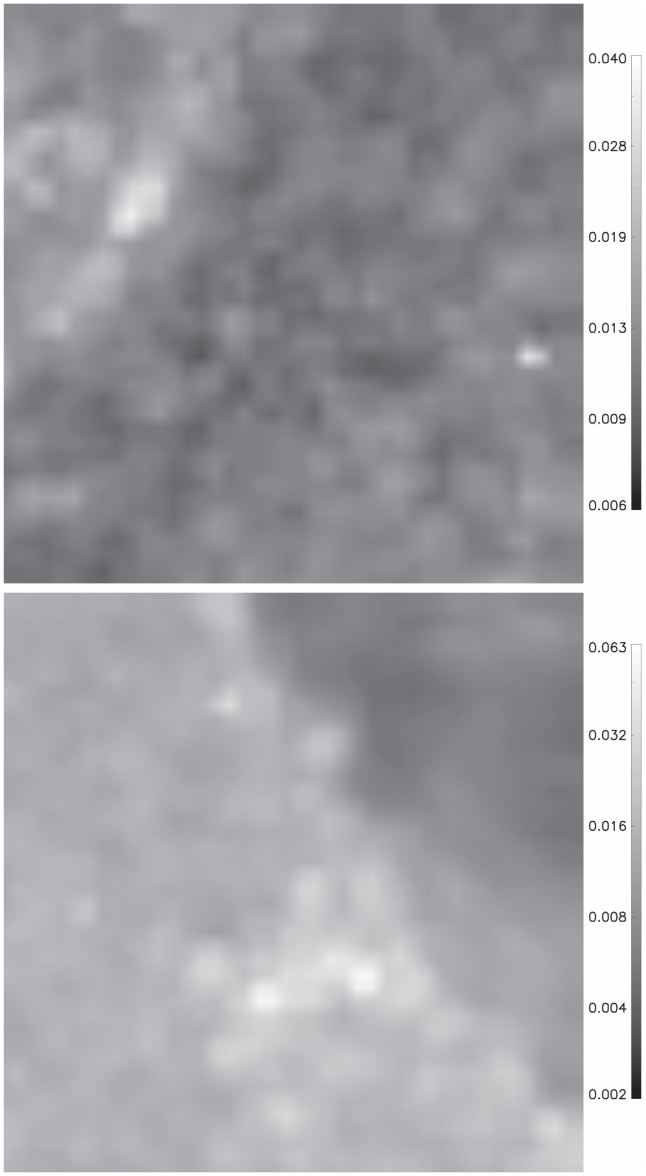

Figure 7. Modeled dust distribution ($E(B - V)$) at the NGP (top) and SGP (bottom). This is to be compared with the 100 μm plots in Figures 1 and 2.

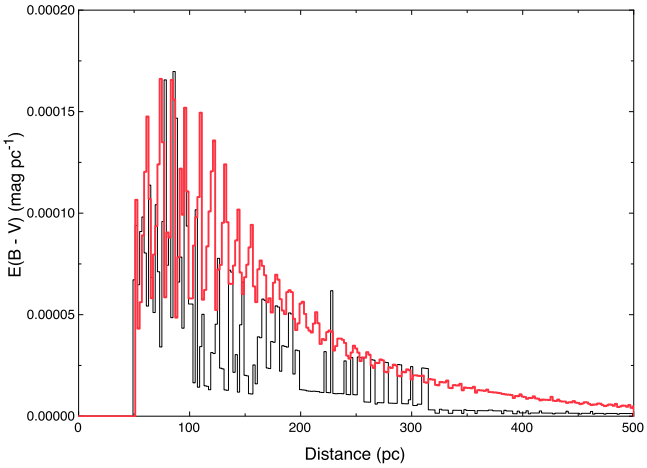

Figure 8. Modeled extinction as a function of distance for the NGP and SGP (red line).

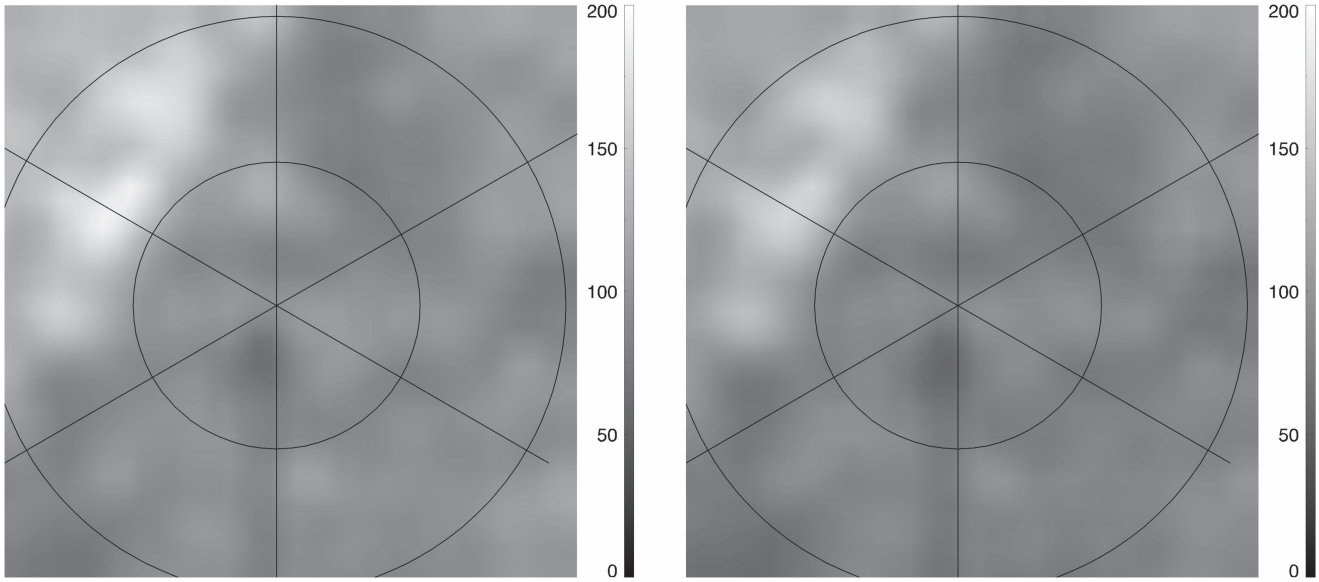

Figure 9. Modeled surface brightness for the NGP in the FUV ($a = 0.4$, $g = 0.6$) and NUV ($a = 0.4$, $g = 0.5$) at a resolution of 30′. The maps are in photon units. The NGP is at the center with lines of latitude at 80° and 85° and lines of longitude every 60° starting from 0° at the top and increasing clockwise.

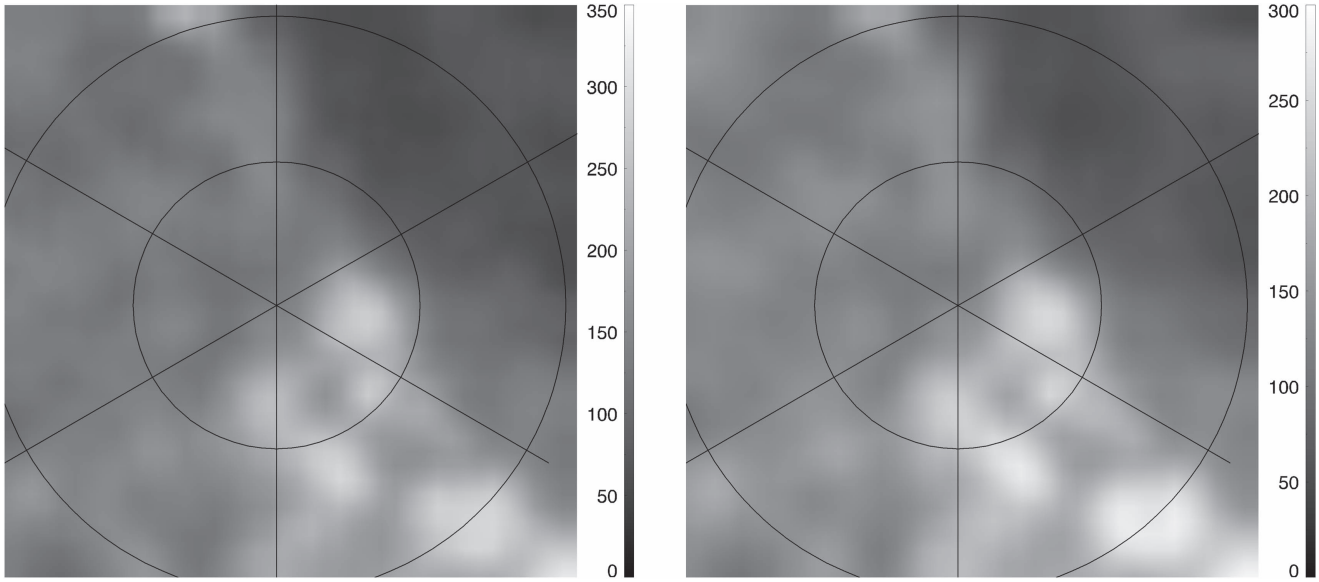

Figure 10. Modeled surface brightness for the SGP in the FUV ($a = 0.4$, $g = 0.6$) and NUV ($a = 0.4$, $g = 0.5$) at a resolution of 30′. The maps are in photon units. The SGP is at the center with lines of latitude at −80° and −85° and lines of longitude every 60° starting from 0° at the top and increasing anticlockwise.

extinction in both poles is low, with minimum values close to zero (McFadzean et al. 1983; Fong et al. 1987), except for limited areas where clouds are seen in the IR maps with peak values of $E(B - V)$ from 0.02 to 0.04 (Berdyugin et al. 2011). Berdyugin et al. (2014) found that the polarization was correlated with the IR maps with the caveat that the polarization maps probed the dust to a distance of about 400 pc while the IR emission measured the dust along the entire line of sight. Berdyugin & Teerikorpi (2016) note that there may be some dusty structures extending to high positive latitudes within Area I, as suggested by the distribution of dark and molecular clouds, in addition to the diffuse dust. In general, we find that our dust model is in agreement with the polarization observations.

We have run our scattering model for a range of optical constants with representative results shown in Figures 9 and 10. The major dust features are clearly visible in the models but the brightness is much less than that observed unless the grains scatter isotropically (Figure 11). Because most of the photons at the poles come from stars in the Galactic plane (Jura 1979), the earliest papers did indeed find that $g = 0$. It is now generally accepted (Draine 2003) that the optical constants are close to $a = 0.4$, $g = 0.6$ in the FUV and $a = 0.4$, $g = 0.5$ in the NUV, and we have used those models to fit the observed emission at each pole. There is too much noise in both the models and the data to compare on a pixel-by-pixel level and we have rather integrated both as a function of the 100 μm values from Schlegel et al. (1998) in Figures 12 and 13.

The fit is good for both poles and both bands, with best-fit offsets of 233 and 234 photon units in the FUV for the NGP and SGP, respectively, and offsets of 485 and 538 photon units in the NUV for the NGP and SGP, respectively. These are not very different from the zero-point offsets in Table 3. We had

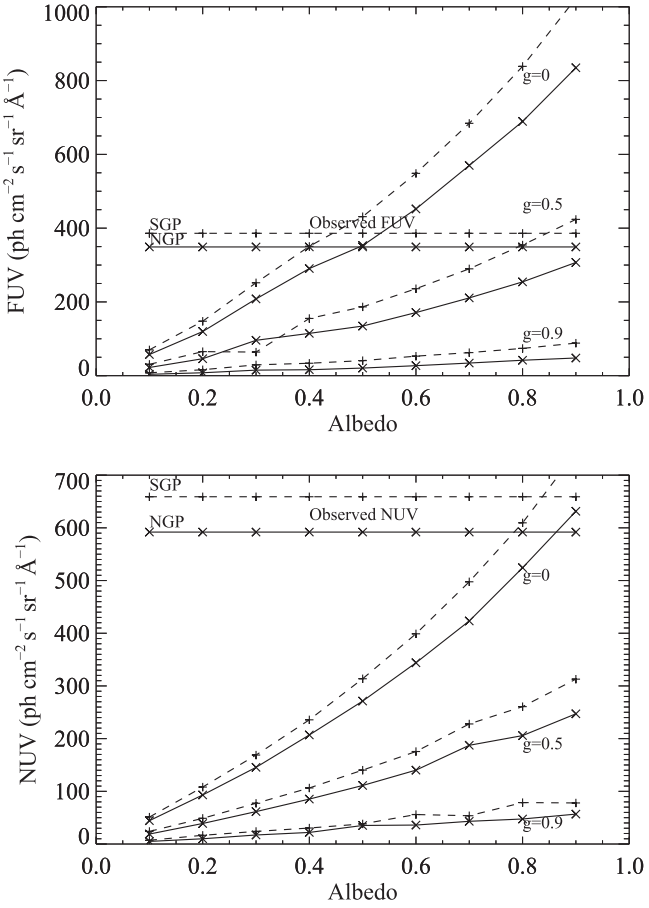

Figure 11. The modeled surface brightness for the NGP (solid line) and the SGP (dashed line) falls short of the observed surface brightness in both the FUV and the NUV. The surface brightness is averaged over the entire region in these plots.

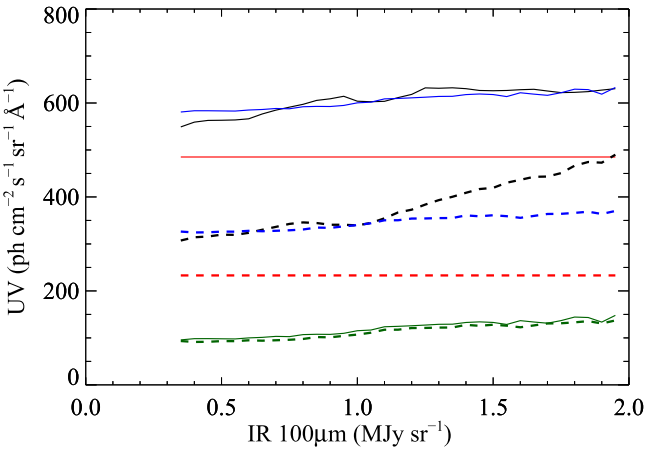

Figure 12. FUV (dashed lines) and NUV (solid lines) modeled surface brightness (green line) plotted against the IR 100 μm surface brightness with the observed background (black line) and the offset (red line) for the NGP. The blue line shows the models with the offsets of 233 photon units in the FUV and 485 photon units in the NUV. The FUV model is for $a = 0.4$ and $g = 0.6$ and the NUV model for $a = 0.4$ and $g = 0.5$.

previously noted the inflection point in the FUV–IR correlation at 1.08 MJy sr^{-1} in the NGP; a comparison with the models shows that it is present for both poles in the FUV. As discussed above, this may be due to fluorescence from the Werner bands of molecular hydrogen.

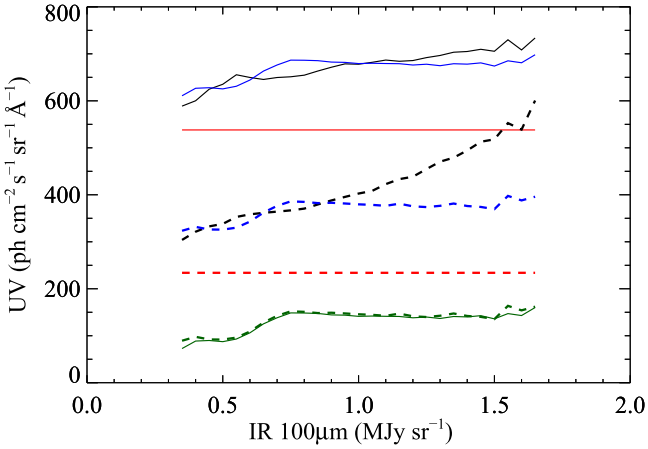

Figure 13. FUV (dashed lines) and NUV (solid lines) modeled surface brightness (green line) plotted against the IR 100 μm surface brightness with the observed background (black line) and the offset (red line) for the SGP. The blue line shows the models with the offsets of 234 photon units in the FUV and 538 photon units in the NUV. The FUV model is for $a = 0.4$ and $g = 0.6$ and the NUV model for $a = 0.4$ and $g = 0.5$.

Table 3
Components of the Background

Component	FUV[a]	NUV[a]
	NGP	
Observed	288 ± 2	531 ± 2
EGL	114 ± 18	194 ± 37
Remainder	174 ± 18	337 ± 37
	SGP	
Observed	241 ± 2	579 ± 3
EGL	114 ± 18	194 ± 37
Remainder	127 ± 18	385 ± 37

Note.
[a] Photon units.

5. Light from Dark Matter?

The continued presence of this unexplained excess in the diffuse background prompts us to briefly consider possible connections to nonstandard physics. Leading particle dark-matter candidates such as supersymmetric weakly interacting massive particles or axions produce photons by annihilation or decay, but not at UV energies (Henry et al. 2015). Another possibility is offered by primordial black holes (PBHs), which emit Hawking radiation with an approximately blackbody spectrum peaking at the characteristic energy $E = \hbar c^3/(8\pi GM)$ for PBHs of mass M. Thus a background with $E = 7$ eV (midway between our FUV and NUV energies) might be associated with PBHs of characteristic mass $M \approx 2 \times 10^{21}$ g. This value coincides with one of three narrow remaining theoretically allowed PBH mass windows (Carr et al. 2016), a so far unremarked coincidence that we find intriguing enough to explore briefly here. A plausible production mechanism for PBHs with masses close to this range has been identified by Espinosa et al. (2018). The question is whether PBHs of this kind could contribute significantly to the unexplained excess identified above, whose bolometric intensity is $Q_u = 4\pi I_\lambda \lambda \approx 5 \times 10^{-5}$ erg s^{-1} cm^{-2} with $I_\lambda \approx 180$ photon units at $\lambda \approx 2000$ Å.

PBH luminosity is very low, $L \lesssim 2 \times 10^{-55} L_{\odot} (M/M_{\odot})^{-2} \approx 6 \times 10^{7}$ erg s^{-1} (Overduin & Wesson 2008). If these PBHs make up the cold dark matter in the halo of the Milky Way, then their local density is $\rho \approx 0.008\, M_{\odot}$ pc^{-3} (Bovy & Tremaine 2012). If they are distributed uniformly, then the nearest one is located at a distance $\bar{r} = (\rho/M)^{-1/3} \approx 100$ au. Its intensity $Q = L/(4\pi\bar{r}^2) \approx 2 \times 10^{-24}$ erg s^{-1} cm^{-2} as seen by us is far too low to account for Q_u. Alternatively, the total number of PBHs in the halo is $N = M_h/M \approx 1 \times 10^{24}$ where $M_h \approx 1 \times 10^{12} M_{\odot}$ (Xue et al. 2008). If these are clustered near the Galactic center at $R = 8$ kpc, then the halo intensity is $Q_h = NL/(4\pi R^2) \approx 2 \times 10^{-19}$ erg s^{-1} cm^{-2}. This is still 15 orders of magnitude too small. More realistically, if the PBH halo extends beyond the Sun and can be regarded as approximately uniform in the solar vicinity, then $Q_h = \mathcal{L}R \approx 7 \times 10^{-17}$ erg s^{-1} cm^{-2} where the luminosity density is $\mathcal{L} = L\rho/M \approx 2 \times 10^{-33}$ erg s^{-1} cm^{-3}. This still falls short of Q_u by 12 orders of magnitude, a discrepancy that cannot plausibly be attributed to non-uniformity in the PBH distribution. We infer that PBHs are not likely to contribute significantly to the astrophysical background, a conclusion reinforced by others (Frampton 2016). The failure of this explanation, of course, only deepens the mystery.

6. Conclusions

We have used *GALEX* data to study the diffuse ultraviolet background at both the north and south Galactic poles with two primary results:

1. There is an excess emission (over the DGL and the EBL) of 120–180 photon units in the FUV and 300–400 photon units in the NUV. Offsets in the UV emission have always been observed at the poles (Table 1) but it has not been apparent how to attribute them to the different contributors. Although we do not know its origin, we can affirm that the excess emission cannot be accounted for by current models of the DGL and EBL.
2. We find that there is a change in the FUV–IR correlation at a 100 μm surface brightness of 1.08 MJy sr^{-1} (Figures 12 and 13). We believe that the most likely explanation for this is molecular hydrogen fluorescence, indicating that self-shielding occurs at a column density of $\log N_H = 20.2$.

We believe that the study of the Galactic poles will prove to be fruitful in differentiating between the Galactic and extragalactic (and terrestrial) components. Deep spectroscopy of the poles, including of cirrus features, would have been invaluable in separating the components but that seems unlikely to be available in the near future with a dearth of UV missions expected. In its absence, we will continue our in-depth study of diffuse emission with *GALEX*.

We thank Prof. Berdyugin and Teerikorpi for clarifying the polarization results at the poles. Part of this research has been supported by the Department of Science and Technology under Grant IR/S2/PU-006/2012. This research has made use of NASA's Astrophysics Data System Bibliographic Services. We have used the Gnu Data Language (http://gnudatalanguage.sourceforge.net/index.php) for the analysis of these data. The data presented in this paper were obtained from the Mikulski Archive for Space Telescopes (MAST). STScI is operated by the Association of Universities for Research in Astronomy, Inc., under NASA contract NAS5-26555. Support for MAST for non-*HST* data is provided by the NASA Office of Space Science via grant NNX09AF08G and by other grants and contracts.

ORCID iDs

M. S. Akshaya https://orcid.org/0000-0001-6258-7474
Jayant Murthy https://orcid.org/0000-0003-4034-5137
S. Ravichandran https://orcid.org/0000-0002-2917-5467
R. C. Henry https://orcid.org/0000-0003-4447-2686
James Overduin https://orcid.org/0000-0002-4760-4130

References

Anderson, R. C., Henry, R. C., Brune, W. H., Feldman, P. D., & Fastie, W. G. 1979, ApJ, 234, 415
Andrews, S. K., Driver, S. P., Davies, L. J. M., Lagos, C. D. P., & Robotham, A. S. G. 2018, MNRAS, 474, 898
Berdyugin, A., Piirola, V., & Teerikorpi, P. 2004, A&A, 424, 873
Berdyugin, A., Piirola, V., & Teerikorpi, P. 2011, in ASP Conf. Ser. 449, Astronomical Polarimetry 2008: Science from Small to Large Telescopes, ed. P. Bastien et al. (San Francisco, CA: ASP), 157
Berdyugin, A., Piirola, V., & Teerikorpi, P. 2014, A&A, 561, A24
Berdyugin, A., Snare, M.-O., & Teerikorpi, P. 1995, A&A, 294, 568
Berdyugin, A., & Teerikorpi, P. 1997, A&A, 318, 37
Berdyugin, A., & Teerikorpi, P. 2002, A&A, 384, 1050
Berdyugin, A., & Teerikorpi, P. 2016, A&A, 587, A79
Berdyugin, A., Teerikorpi, P., & Haikala, L. 2000, A&A, 358, 717
Berdyugin, A., Teerikorpi, P., Haikala, L., et al. 2001, A&A, 372, 276
Bevington, P. R., & Robinson, D. K. 2003, Data Reduction and Error Analysis for the Physical Sciences, (Boston, MA: McGraw-Hill)
Boissier, S., Boselli, A., Voyer, E., et al. 2015, A&A, 579, A29
Bovy, J., & Tremaine, S. 2012, ApJ, 756, 89
Bowyer, S. 1991, ARA&A, 29, 59
Carr, B., Kühnel, F., & Sandstad, M. 2016, PhRvD, 94, 083504
Castelli, F., & Kurucz, R. L. 2004, arXiv:astro-ph/0405087
Draine, B. T. 2003, ARA&A, 41, 241
Driver, S. P., Andrews, S. K., Davies, L. J., et al. 2016, ApJ, 827, 108
Espinosa, J. R., Racco, D., & Riotto, A. 2018, PhRvL, 120, 121301
Feldman, P. D., Brune, W. H., & Henry, R. C. 1981, ApJL, 249, L51
Fong, R., Jones, L. R., Shanks, T., Stevenson, P. R. F., & Strong, A. W. 1987, MNRAS, 224, 1059
Frampton, P. H. 2016, MPLA, 31, 1650093
Franco, J., & Cox, D. P. 1986, PASP, 98, 1076
Gardner, J. P., Brown, T. M., & Ferguson, H. C. 2000, ApJL, 542, L79
Gillmon, K., Shull, J. M., Tumlinson, J., & Danforth, C. 2006, ApJ, 636, 891
Green, G. M., Schlafly, E. F., Finkbeiner, D. P., et al. 2015, ApJ, 810, 25
Hamden, E. T., Schiminovich, D., & Seibert, M. 2013, ApJ, 779, 180
Henry, R. C. 1991, ARA&A, 29, 89
Henry, R. C., & Murthy, J. 1993, ApJL, 418, L17
Henry, R. C., Murthy, J., Overduin, J., & Tyler, J. 2015, ApJ, 798, 14
Henyey, L. G., & Greenstein, J. L. 1941, ApJ, 93, 70
Hill, R., Masui, K. W., & Scott, D. 2018, arXiv:1802.03694
Hurwitz, M. 1998, ApJL, 500, L67
Jakobsen, P., Bowyer, S., Kimble, R., et al. 1984, A&A, 139, 481
Jo, Y.-S., Seon, K.-I., Min, K.-W., Edelstein, J., & Han, W. 2017, ApJS, 231, 21
Joubert, M., Deharveng, J. M., Cruvellier, P., Masnou, J. L., & Lequeux, J. 1983, A&A, 128, 114
Jura, M. 1979, ApJ, 227, 798
Kashikawa, N., Shimasaku, K., Yasuda, N., et al. 2004, PASJ, 56, 1011
Knapp, G. R. 1974, AJ, 79, 527
Lagache, G., Haffner, L. M., Reynolds, R. J., & Tufte, S. L. 2000, A&A, 354, 247
Ly, C., Malkan, M. A., Treu, T., et al. 2009, ApJ, 697, 1410
Madau, P. 1992, ApJL, 389, L1
Markkanen, T. 1979, A&A, 74, 201
Marshall, D. J., Robin, A. C., Reylé, C., Schultheis, M., & Picaud, S. 2006, A&A, 453, 635
Martin, C., Hurwitz, M., & Bowyer, S. 1991, ApJ, 379, 549
Martin, D. C., Fanson, J., Schiminovich, D., et al. 2005, ApJL, 619, L1
Matsuoka, Y., Ienaka, N., Kawara, K., & Oyabu, S. 2011, ApJ, 736, 119
McFadzean, A. D., Hilditch, R. W., & Hill, G. 1983, MNRAS, 205, 525

Morrissey, P., Conrow, T., Barlow, T. A., et al. 2007, ApJS, 173, 682
Murthy, J. 2014a, ApJS, 213, 32
Murthy, J. 2014b, Ap&SS, 349, 165
Murthy, J. 2016, MNRAS, 459, 1710
Murthy, J., & Henry, R. C. 1995, ApJ, 448, 848
Murthy, J., Henry, R. C., & Sujatha, N. V. 2010, ApJ, 724, 1389
Onaka, T., & Kodaira, K. 1991, ApJ, 379, 532
Overduin, J. M., & Wesson, P. S. 2008, The Light/Dark Universe: Light from Galaxies, Dark Matter and Dark Energy (Singapore: World Scientific)
Paresce, F., Bowyer, S., Lampton, M., & Margon, B. 1979, ApJ, 230, 304
Paresce, F., McKee, C. F., & Bowyer, S. 1980, ApJ, 240, 387
Perryman, M. A. C., Lindegren, L., Kovalevsky, J., et al. 1997, A&A, 323, L49
Planck Collaboration, Abergel, A., Ade, P. A. R., et al. 2014, A&A, 571, A11
Reach, W. T., Koo, B.-C., & Heiles, C. 1994, ApJ, 429, 672
Savage, B. D., Bohlin, R. C., Drake, J. F., & Budich, W. 1977, ApJ, 216, 291
Schlegel, D. J., Finkbeiner, D. P., & Davis, M. 1998, ApJ, 500, 525
Tennyson, P. D., Henry, R. C., Feldman, P. D., & Hartig, G. F. 1988, ApJ, 330, 435
Voyer, E. N., Gardner, J. P., Teplitz, H. I., Siana, B. D., & de Mello, D. F. 2011, ApJ, 736, 80
Wakker, B. P. 2006, ApJS, 163, 282
Welsh, B. Y., Lallement, R., Vergely, J.-L., & Raimond, S. 2010, A&A, 510, A54
Xu, C. K., Donas, J., Arnouts, S., et al. 2005, ApJL, 619, L11
Xue, X. X., Rix, H. W., Zhao, G., et al. 2008, ApJ, 684, 1143